J. Fluid Mech. (1969), *vol.* 38, *part* 4, *pp.* 713–720
Printed in Great Britain

On the dynamic motion of a thin flexible cylinder in a viscous stream

By C. R. ORTLOFF AND J. IVES

General Research Corporation, 6300 Hollister Avenue, P.O. Box 3587, Santa Barbara, California 93105

(Received 7 March 1969)

The stability and time-dependent deflexions of a thin flexible cylinder with zero bending rigidity set in a viscous stream are examined. The cylinder is fixed at one end and free at the other. Modal shapes are found based on solutions to linearized equations resulting from small deflexion assumptions; the dependence of cylinder motion upon the aerodynamic, elastic and physical size characteristics of the cylinder is exhibited. It is found that the cylinder motion is always unstable and that cylinder amplitude increases without bound as time is increased.

1. Introduction

In a previous study, Paidoussis (1966*a*, *b*) numerically analyzed the dynamic motion of a thin flexible finite-length cylinder fixed at one end and free at the other end and immersed in a viscous fluid stream. The time-dependent instability of the cylinder was shown to be dependent upon the elastic, aerodynamic and physical size properties of the cylinder for cases in which the bending stiffness (EI) was bounded away from zero. The quantity E is Young's modulus and I is the cylinder cross-section moment of inertia. Cylinder motions were assumed small, thus permitting linearization assumptions in the governing differential equations. For the special case of zero EI or, equivalently, an infinitely flexible cylinder, special function solutions for the time-dependent cylinder motion may be found under the assumptions of small cylinder deflexions and vibration frequency. This case provides a good approximation to the dynamic motion of very thin, long wires whose bending rigidity is small (owing to the small cross-sectional moment of inertia which varies as the wire diameter to the fourth power). Previously, the similar problem of the flapping flag given by Lamb (1932, p. 374) (which is also a zero bending rigidity plane surface) has been analyzed; the present analysis extends such work to cylinder dynamic motions and presents results on cylinder stability and displacement in terms of special function solutions.

Initially the equations governing cylinder motion in a viscous fluid stream are briefly reviewed. Subsequently, the equation for the zero bending rigidity case is obtained as a special case of the general equation. Finally, solutions for modal shapes and deflexion amplitudes of the zero bending rigidity cylinder are given as functions of cylinder aerodynamic and mechanical properties.

2. Equations of motion of a wire suspended in a fluid stream

Following Paidoussis (1966*a*, *b*) and Gregory & Paidoussis (1966) the equations governing the motion of a flexible wire fixed at one end, free at the other end and immersed in a uniform stream are

$$\frac{\partial T}{\partial x} + F_L = 0, \tag{1}$$

$$\frac{\partial Q}{\partial x} - F_N - M\left(\frac{\partial}{\partial t} + U\frac{\partial}{\partial x}\right)^2 y - m\frac{\partial^2 y}{\partial t^2} + \frac{\partial}{\partial x}\left(T\frac{\partial y}{\partial x}\right) = 0, \tag{2}$$

where $T = T(x,t)$ is the local value of the tension induced by aerodynamic shear and pressure forces, Q is the shear force normal to the wire axis, M is the lateral virtual mass of fluid per unit length of wire accelerated by the accelerating wire, m is the mass of the wire per unit length, and U is the velocity of the free stream. Equations (1) and (2) represent the longitudinal and normal force

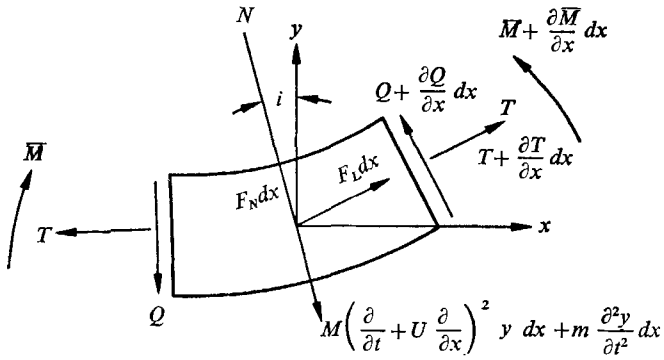

FIGURE 1. Force balance on an element of wire.

balance equations acting on an element of wire (figure 1). It is to be noted that (1) and (2) have been linearized with respect to small angular wire deflexions. The terms F_L and F_N represent aerodynamic contributions representing the lateral shear force and normal pressure forces per unit length respectively; $\bar{M}$ is the bending moment and $Q = -\partial\bar{M}/\partial x - EI\,\partial^3 y/\partial x^3$. The quantity y is the vertical displacement, x is distance along the unperturbed wire axis and t is time. The origin $x = y = 0$ of the wire is located at the fixed end. Note that, when aerodynamic and shear forces are absent, (1) and (2) reduce to the wave equation for a string with constant tension. Further assumptions regarding the derivation of (1) and (2) are listed in Paidoussis (1966*a*).

Drag data for roughened cylinders have been summarized by Taylor (1952) for Reynolds number (R) flows characteristic of turbulent flow conditions. Briefly, for roughened cylinders

$$\left.\begin{aligned} F_N &= \frac{2}{\pi}\frac{M}{D}U^2\{C_{D_p}\sin^2 i + C_f \sin i\}, \\ F_L &= \frac{2}{\pi}\frac{M}{D}U^2 C_f \cos i, \end{aligned}\right\} \tag{3}$$

where C_{D_p} and C_f are the drag coefficients due to pressure and shear forces acting on the wire surface. The fluid density ρ was eliminated by $\rho = 4M/\pi D^2$, where D is the wire diameter. The F_N and F_L expressions given in (3) are essentially propositions in which the C_{D_p} and C_f values are empirically selected from experimental data taken from turbulent-boundary-layer-induced forces on inclined roughened cylinders. The roughness pattern is one of a large number of projections normal to the cylinder. The angle i is given by

$$i = \sin^{-1}\frac{v}{U} = \sin^{-1}\left[\left(\frac{\partial y}{\partial t} + U\frac{\partial y}{\partial x}\right)U^{-1}\right],$$

where the quantity v is the velocity component in the y direction. For small wire motions, i is small† so that (3) becomes, for turbulent boundary-layer flow over roughened wall cylinders,

$$F_N \simeq \frac{1}{2}\frac{M}{D}UC_N\left(\frac{\partial y}{\partial t} + U\frac{\partial y}{\partial x}\right), \quad F_L \simeq \frac{1}{2}\frac{M}{D}U^2C_T, \tag{4}$$

where $C_N = (4/\pi)C_{D_p}$ and $C_T = (4/\pi)C_f$ and terms of the order of i^2 have been neglected. From (1) and (4) the wire tension is, for a roughened wall wire (of total length L),

$$T(x) = \frac{1}{2}\frac{M}{D}U^2C_T(L-x). \tag{5}$$

Combining (1), (2), (4) and (5), the governing equation of motion for a roughened surface wire is

$$EI\frac{\partial^4 y}{\partial x^4} + (M+m)\frac{\partial^2 y}{\partial t^2} + MU^2\frac{\partial^2 y}{\partial x^2} + 2MU\frac{\partial^2 y}{\partial t\,\partial x} - \frac{\partial}{\partial x}\left[\frac{C_T}{2}\left(\frac{M}{D}\right)U^2(L-x)\frac{\partial y}{\partial x}\right] + \tfrac{1}{2}C_N\frac{M}{D}U\left(\frac{\partial y}{\partial t} + U\frac{\partial y}{\partial x}\right) = 0. \tag{6}$$

3. Special case of the zero bending rigidity wire

From (6) the special case of the zero bending rigidity (or an infinitely flexible) cylinder is obtained by setting $EI = 0$. The governing equation for the amplitude of the roughened surface cylinder under the influence of turbulent-boundary-layer-induced forces is

$$\frac{\partial^2 y}{\partial t^2}\frac{M+m}{M} + \frac{\partial^2 y}{\partial x^2}\left[U^2 - \tfrac{1}{2}C_T\frac{U^2}{D}(L-x)\right] + \frac{\partial y}{\partial x}\frac{U^2}{2D}(C_T + C_N) + 2U\frac{\partial^2 y}{\partial x\,\partial t} + \tfrac{1}{2}C_N\frac{U}{D}\frac{\partial y}{\partial t} = 0. \tag{7}$$

With the non-dimensionalization

$$\tau = (t/L)U, \quad \beta = M/(M+m),$$
$$\xi = x/L, \quad \epsilon = L/D, \quad \eta = y/L,$$

the above equation becomes

$$\frac{\partial^2 \eta}{\partial \tau^2} + \frac{\partial^2 \eta}{\partial \xi^2}\beta[1 - \tfrac{1}{2}C_T\epsilon(1-\xi)] + \frac{\partial \eta}{\partial \xi}\frac{(C_T + C_N)\epsilon\beta}{2} + 2\beta\frac{\partial^2 \eta}{\partial \xi\,\partial \tau} + \tfrac{1}{2}C_N\epsilon\beta\frac{\partial \eta}{\partial \tau} = 0, \tag{8}$$

† The motion of a fluid element, following its passage in time along the wire surface, is such that only small deviations from a horizontal path are permitted in accordance with linearization assumptions.

while the boundary and initial conditions become

$$\left.\begin{array}{ll} \eta = 0; & \xi = 0 \text{ (fixed end condition);} \\ |\eta| \text{ is finite;} & \xi = 1 \text{ (bounded free-end deflexion);} \\ \partial\eta/\partial\tau = 0; & \tau = 0 \text{ (zero initial velocity);} \\ \eta = \eta_1(\xi); & \tau = 0 \text{ (prescribed initial deflexion).} \end{array}\right\} \quad (9a, b, c, d)$$

With the further notation

$$a = \beta(1-\tfrac{1}{2}C_T\epsilon) = \beta(1-b), \quad c = \tfrac{1}{2}(C_T+C_N)\epsilon\beta = b+d,$$
$$b = \tfrac{1}{2}\beta C_T\epsilon, \qquad\qquad d = \tfrac{1}{2}C_N\epsilon\beta,$$

and the change of independent variable $a+b\xi = \mu$, (8) becomes

$$\frac{\partial^2\eta}{\partial\tau^2} + \mu b^2\frac{\partial^2\eta}{\partial\mu^2} + bc\frac{\partial\eta}{\partial\mu} + 2\beta b\frac{\partial^2\eta}{\partial\tau\,\partial\mu} + d\frac{\partial\eta}{\partial\tau} = 0. \quad (10)$$

Letting $\eta = e^{i\omega\tau}v(\mu)$ and then with the independent variable change $z^2 = \mu$, (10) finally becomes Bessel's equation

$$z^2\frac{d^2v}{dz^2} + z\frac{dv}{dz}\left[\frac{2}{b}(c+2\beta i\omega) - 1\right] + z^2v\frac{4\omega}{b^2}(id-\omega) = 0, \quad (11)$$

with the general solution for non-integer indices

$$v(z) = z^{\mathbf{p}}\left\{AJ_{\mathbf{p}}\left[\pm\left(\frac{\omega^2-di\omega}{b^2}\right)^{\frac{1}{2}}2iz\right] + BJ_{-\mathbf{p}}\left[\pm\left(\frac{\omega^2-di\omega}{b^2}\right)^{\frac{1}{2}}2iz\right]\right\}, \quad (12)$$

where

$$\mathbf{p} = 1-\frac{C_T+C_N}{C_T}-\frac{4i\omega}{C_T\epsilon} = -\frac{C_N}{C_T}-\frac{4i\omega}{C_T\epsilon},$$

or, in terms of the original variables, assuming non-integer indices,

$$v(\xi) = (a+b\xi)^{\frac{1}{2}\mathbf{p}}\left\{AJ_{\mathbf{p}}\left[\pm\left(\frac{\omega^2-di\omega}{b^2}\right)^{\frac{1}{2}}2(a+b\xi)^{\frac{1}{2}}i\right] + BJ_{-\mathbf{p}}\left[\pm\left(\frac{\omega^2-di\omega}{b^2}\right)^{\frac{1}{2}}2(a+b\xi)^{\frac{1}{2}}i\right]\right\}, \quad (13)$$

where A and B are constants to be determined from boundary and initial conditions. The quantity $J_\nu(z)$ is the Bessel function of the first kind of index ν and argument z.

Consistent with the thin cylinder assumption is the fact that $\epsilon \gg 1$ (for purposes of this discussion, $\epsilon\to\infty$). Without loss of generality, it is assumed that the product $\epsilon\beta$ is bounded; then the above may be approximated† by

$$v(\xi, \epsilon\to\infty) \simeq (a+b\xi)^{-C_N/2C_T}\left\{AJ_{-C_N/C_T}\left[\pm\omega^{\frac{1}{2}}\left(-\frac{a}{b}-\xi\right)^{\frac{1}{2}}2b^{-\frac{1}{2}}(\omega-id)^{\frac{1}{2}}\right] + BJ_{C_N/C_T}\left[\pm\omega^{\frac{1}{2}}\left(-\frac{a}{b}-\xi\right)^{\frac{1}{2}}2b^{-\frac{1}{2}}(\omega-id)^{\frac{1}{2}}\right]\right\}. \quad (14)$$

† The condition of $\epsilon \gg 4\omega/C_T$ is also implied in the neglect of the complex term in the imaginary part of the complex index. The condition of ω small implies that the first few eigensolutions contribute most to the modal shape. The *a posteriori* confirmation of this may be seen in figures 2–4, where wire amplitudes (formed from the sum of 10^2 eigensolutions) are composed of lower modes. Physically, the *a priori* assumption of ω small is meaningful in that instability is usually manifested in lower-modal shapes first and then progresses to higher-modal shapes. The assumption of small ω is also consistent with v/U small so that the small wire deflexion theory (§2) holds.

Assume† next that $C_N/C_T = \frac{1}{2}$; further, as $|v|$ is to be finite at $\xi = 1$, application of L'Hôspital's rule to the previous equation for $\xi \to -a/b \simeq 1$ as $\epsilon \to \infty$ leads to

$$v(\xi) \simeq (a+b\xi)^{-\frac{1}{4}} B J_{\frac{1}{2}}\left[\pm 2\omega^{\frac{1}{2}}\left(-\frac{a}{b}-\xi\right)^{\frac{1}{2}} b^{-\frac{1}{2}}(\omega - id)^{\frac{1}{2}}\right] \quad (0 \leqslant \xi \leqslant 1). \tag{15}$$

The condition of $v(0) = 0$ then requires that

$$\pm 2\omega_n^{\frac{1}{2}}(-a/b)^{\frac{1}{2}} b^{-\frac{1}{2}}(\omega_n - id)^{\frac{1}{2}} = \delta_n,$$

where δ_n are the zeros of the Bessel function in (15). The positive zeros are given by

$$\delta_n = n\pi \quad (n = 0, 1, 2, \ldots).$$

The ω_n is then given by‡

$$\omega_n \simeq \frac{id}{2} \pm \frac{1}{2}\left(-\frac{b^2}{a}\delta_n^2 - d^2\right)^{\frac{1}{2}}. \tag{16}$$

Therefore, assuming zero initial velocity of the cylinder at $\tau = 0$,

$$\eta(\xi,\tau) \simeq R\left\{\left(-\frac{a}{b}-\xi\right)^{-\frac{1}{4}}(-b)^{-\frac{1}{4}} \sum_{n=1}^{\infty} B_n (\cos\omega_n\tau) \times J_{\frac{1}{2}}\left[\pm 2\omega_n^{\frac{1}{2}}\left(-\frac{a}{b}-\xi\right)^{\frac{1}{2}} b^{-\frac{1}{2}}(\omega_n - id)^{\frac{1}{2}}\right]\right\}. \tag{17}$$

The remaining initial condition necessary to fix B_n is the prescribed initial deflexion $\eta = \eta_1(\xi, \tau = 0)$. To this end, assume $\eta_1(\xi)$ may be expanded as

$$\eta_1(\phi) = \sum_{n=1}^{\infty} \Omega_n J_{\frac{1}{2}}(u_n\phi),$$

where u_n are the successive positive roots of $J_{\frac{1}{2}}(u) = 0$ and Ω_n are coefficients independent of ϕ. Then, as

$$\frac{2}{J_{\frac{3}{2}}^2(u_n)} \int_0^1 \phi J_{\frac{1}{2}}(u_n\phi)\,\eta_1(\phi)\,d\phi = \Omega_n$$

and

$$\int_0^1 \phi J_{\frac{1}{2}}(\sigma_p\phi)\,J_{\frac{1}{2}}(\sigma_q\phi)\,d\phi = 0 \quad (\sigma_p \neq \sigma_q)$$

where σ_p, σ_q are any two roots of $J_{\frac{1}{2}}(u) = 0$, then the expression for $\eta_1(\phi)$ may be expanded in an orthonormal set. Let

$$\eta_1(\phi) = h\left(-\frac{a}{b}-\xi\right)^{-\frac{1}{4}} \xi^{\lambda}\left(-\frac{a}{b}-\xi\right)^{\gamma},$$

† For the large-scale surface roughness patterns discussed by Taylor (1952) (figure 2 of Taylor in particular specifies a roughness pattern for which (3) is valid), cases for which $C_N/C_T < 1$ are feasible. Based on results from Taylor, the physically realizable range for C_N/C_T is on the order of $\frac{1}{2} \lesssim C_N/C_T \lesssim 2$, where $C_N/C_T \simeq 2$ holds for smooth cylinders and $C_N/C_T \simeq \frac{1}{2}$ for very rough cylinders. For small wall roughness, Paidoussis (1966*a*, *b*) used $C_N/C_T = 1$. From a mathematical point of view, a bounded solution may be obtained (for $\epsilon \gg 1$) for $C_N/C_T \geqslant \frac{1}{2}$; the limit for which rough cylinder theory applies is then probably on the order of $\frac{1}{2} \leqslant C_N/C_T = 1$.

‡ The negative sign is selected from this point forward so that $\omega_0 = 0$ corresponds to $\eta = 0$.

where $\lambda > 0$, $\gamma \geqslant \frac{1}{4}$, and $0 \leqslant |h| \leqslant 1$, where h is a scale factor in the expression for the initial displacement. Then it follows that as $u_n = \pm 2\omega_n^{\frac{1}{2}} b^{-\frac{1}{2}}(\omega_n - id)^{\frac{1}{2}}$ then $\phi = [-(a/b)-\xi]^{\frac{1}{2}}$, where $0 \leqslant \phi \leqslant 1$. Then

$$\left.\begin{aligned}\eta(\xi,\tau) \simeq R\Bigg\{(-b)^{-\frac{1}{4}}\left(-\frac{a}{b}-\xi\right)^{-\frac{1}{4}} h \sum_{n=1}^{\infty} \frac{2\cos\omega_n\tau}{J_{\frac{1}{2}}^2[\pm 2\omega_n^{\frac{1}{2}} b^{-\frac{1}{2}}(\omega_n - id)^{\frac{1}{2}}]} \\ \times J_{\frac{1}{2}}\left[\pm 2\omega_n^{\frac{1}{2}}\left(-\frac{a}{b}-\xi\right)^{\frac{1}{2}} b^{-\frac{1}{2}}(\omega_n - id)^{\frac{1}{2}}\right]\int_0^1 \left(-\frac{a}{b}-\xi\right)^{\frac{1}{2}} \\ \times J_{\frac{1}{2}}\left[\pm \omega_n^{\frac{1}{2}} b^{-\frac{1}{2}}(\omega_n - id)^{\frac{1}{2}} 2\left(-\frac{a}{b}-\xi\right)^{\frac{1}{2}}\right]\xi^{\lambda}\left(-\frac{a}{b}-\xi\right)^{\lambda} d\left(-\frac{a}{b}-\xi\right)^{\frac{1}{2}}\Bigg\}.\end{aligned}\right\} \tag{18}$$

In the last integral, let $[-(a/b)-\xi]^{\frac{1}{2}} = t$ so that the above integral becomes

$$(-1)^{\lambda}\int_0^1 J_{\frac{1}{2}}[\pm 2\omega_n^{\frac{1}{2}} b^{-\frac{1}{2}}(\omega_n - id)^{\frac{1}{2}} t]\, t^{2\gamma+1}\left(t^2+\frac{a}{b}\right)^{\lambda} dt = I_n.$$

Suppose that $\lambda = 1$, $\gamma = \frac{1}{2}$, then it follows that (Luke 1962, p. 51)

$$-I_n = 4\frac{\alpha_n^{-1}}{11}\sum_{k=0}^{\infty}\frac{(\frac{3}{2}+2k)(-\frac{5}{4})_k}{(\frac{15}{4})_k} J_{\frac{3}{2}+2k}(\alpha_n) + 2\frac{a}{b}\frac{\alpha_n^{-1}}{7}\sum_{k=0}^{\infty}\frac{(\frac{3}{2}+2k)(-\frac{1}{4})_k}{(\frac{11}{4})_k} J_{\frac{3}{2}+2k}(\alpha_n), \tag{19}$$

where $$\alpha_n = \pm 2\omega_n^{\frac{1}{2}} b^{-\frac{1}{2}}(\omega_n - id)^{\frac{1}{2}},$$

and $$(a)_k = \Gamma(a+k)/\Gamma(a).$$

Finally, using (18) and (19) the deflexion becomes

$$\left.\begin{aligned}\eta(\xi,\tau) \simeq R\Bigg(-(-b)^{-\frac{1}{4}} h\left(-\frac{a}{b}-\xi\right)^{-\frac{1}{4}} \sum_{n=1}^{\infty}\frac{2\cos\omega_n\tau}{J_{\frac{3}{2}}^2\{\delta_n[-b/a]^{\frac{1}{2}}\}} \\ \times J_{\frac{1}{2}}\left[\left(-\frac{b}{a}\right)^{\frac{1}{2}}\delta_n\left(-\frac{a}{b}-\xi\right)^{\frac{1}{2}}\right]\left\{\frac{4}{11}\delta_n^{-1}\left(-\frac{b}{a}\right)^{\frac{1}{2}}\sum_{k=0}^{\infty}\frac{(\frac{3}{2}+2k)(-\frac{5}{4})_k}{(\frac{15}{4})_k} J_{\frac{3}{2}+2k}\left[\delta_n\left(-\frac{b}{a}\right)^{\frac{1}{2}}\right]\right. \\ \left.+\frac{2}{7}\left(\frac{a}{b}\right)\delta_n^{-1}\left(-\frac{b}{a}\right)^{-\frac{1}{2}}\sum_{k=0}^{\infty}\frac{(\frac{3}{2}+2k)(-\frac{1}{4})_k}{(\frac{11}{4})_k} J_{\frac{3}{2}+2k}\left[\delta_n\left(-\frac{b}{a}\right)^{\frac{1}{2}}\right]\right\}\Bigg).\end{aligned}\right\} \tag{20}$$

Note that for increasing τ the amplitude is always increasing for large ϵ case (large L/D) as ω_n is always complex; the wire is unstable for such cases. This is in qualitative agreement with results of Paidoussis, who showed that large $u = (M/EI)^{\frac{1}{2}}UL$ leads to instability. Also, the planar problem of the flapping flag treated by Lamb (1945) is analogous in that the amplitude of motion continually increases for increasing time as in the present problem of cylinder motion.

4. Discussion of results

Some sample calculations obtained from (20) are shown in figures 2–4. The first result, shown in figure 2, is the cylinder deflexion for $\tau = 10^{-2}$, $\beta = 10^{-3}$ and $\epsilon = 20$. Although the assumption of $\epsilon \gg 1$ necessary in the derivation of (7) may not be fully met by $\epsilon = 20$, nevertheless the condition of $\epsilon \gg 4\omega/C_T$ is met (*a posteriori*) owing to the low modal shape resulting from the first 10^2 eigensolutions in (20).

Figure 2 indicates a low modal shape characteristic of low ϵ shapes. A nodal point appears at $\xi \simeq 0{\cdot}75$. Typical maximum amplitudes are on the order of $\eta \simeq 7h \times 10^{-3}$ for non-dimensional times on the order of $\tau = 10^{-2}$.

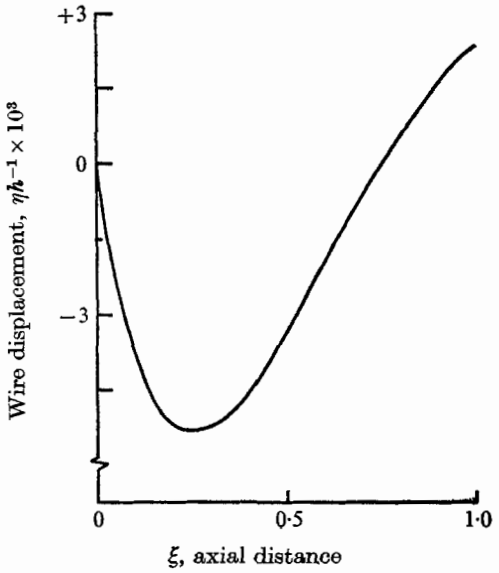

FIGURE 2. Wire displacement *vs.* axial distance for $\tau = 10^{-2}, \beta = 10^{-3}, \epsilon = 20$ for $EI = 0$.

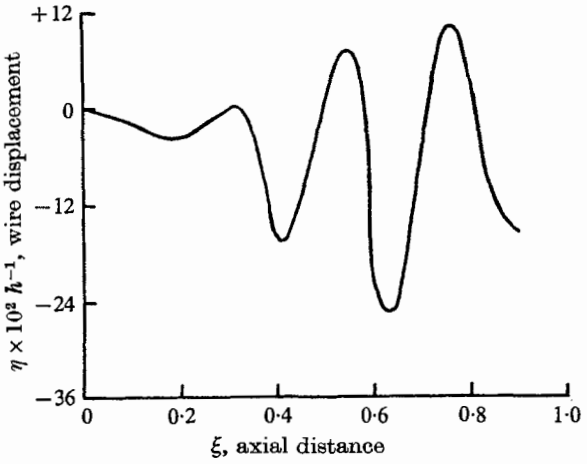

FIGURE 3. Wire displacement *vs.* axial distance for $\tau = 10^{-2}, \beta = 10^{-3}, \epsilon = 10^5$ for $EI = 0$.

Figure 3 illustrates cylinder amplitude for $\beta = 10^{-3}$, $\epsilon = 10^5$ and $\tau = 10^{-2}$; figure 4 illustrates cylinder amplitude for similar conditions except that $\beta = 2{\cdot}17 \times 10^{-8}$. Comparison of figures 3 and 4 indicates that decreasing β (for fixed ϵ) results in increasing cylinder amplitudes for the same τ value. For example, decreasing β from 10^{-3} to $2{\cdot}17 \times 10^{-8}$ results in a scale change of 100 in amplitude. Additionally, a decrease in β results in an apparent shape change from one containing many modal points (figure 3) to one of many higher harmonics super-

imposed upon a lower harmonic with a single nodal point (figure 4). Similarly, an increase in ϵ for fixed τ and β results in basically more complex modal shapes as may be seen by comparison of figure 2 with figure 3. Effects of ϵ changes (for fixed β and τ) are also shown in figure 4. A decrease in ϵ from 10^5 to $\epsilon = 4{\cdot}28 \times 10^3$

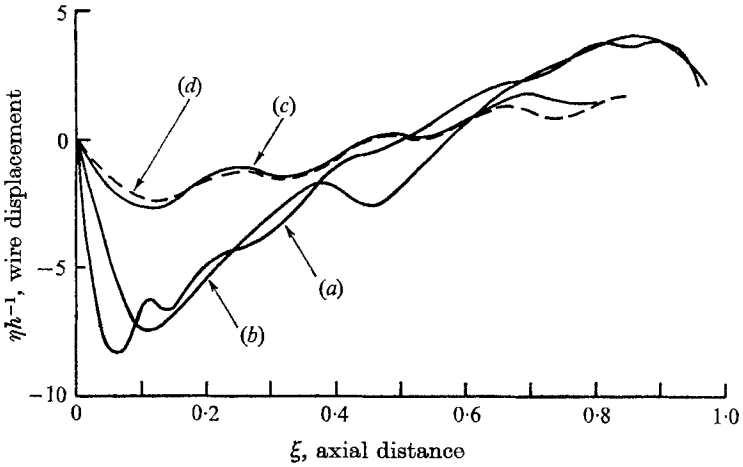

FIGURE 4. Wire displacement *vs.* axial distance for $\beta = 2{\cdot}17 \times 10^{-8}$ for various τ and ϵ values and for $EI = 0$. (*a*) $\tau = 1$, $\epsilon = 4{\cdot}28 \times 10^3$; (*b*) $\tau = 10^{-2}$, $\epsilon = 4{\cdot}28 \times 10^3$; (*c*) $\tau = 10^{-2}$, $\epsilon = 10^5$; (*d*) $\tau = 1$, $\epsilon = 10^5$.

(figures 3, 4) is seen to result in a lessening of maximum cylinder amplitude by approximately a factor of 2 for fixed β; a decrease in ϵ from 10^5 to 20 (figures 2, 3) results in a decrease in maximum cylinder amplitude of approximately a factor of 100. Effects of increasing τ are to increase amplitude without bound for all cases studied. It may be concluded that cylinder motion is always unstable with increasing τ. The problem of the flapping flag treated by Lamb (1945) is analogous in that for the planar problem the amplitude of motion continually increased for increasing time (or τ) as in the present problem. Although the zero bending rigidity cases are characterized by instability, the short time cylinder shapes are dependent strongly on parameters used to characterize the physical and mechanical properties of the cylinder. For the long time amplitudes and deflexions (which may be characterized by large deflexions and as such fall outside of the range of applicability of linearized small deflexion theory), non-linear theory must be employed to answer questions as to whether or not the amplitude is bounded.

REFERENCES

GREGORY, R. W. & PAIDOUSSIS, M. P. 1966 *Proc. Roy. Soc.* A **293**, 512.

LAMB, H. 1945 *Hydrodynamics*, 6th ed. New York: Dover.

LUKE, Y. L. 1962 *Integrals of Bessel Functions*. New York: McGraw-Hill.

PAIDOUSSIS, M. P. 1966*a* *J. Fluid Mech.* **26**, 717.

PAIDOUSSIS, M. P. 1966*b* *J. Fluid Mech.* **26**, 737.

TAYLOR, G. I. 1952 *Proc. Soc. Roy.* A **214**, 158.